

D.V. Lal^{1,4}, M.J. Hardcastle², R.P. Kraft³, A.P. Rao⁴

¹*Max-Planck-Institut für Radioastronomie, Auf dem Hügel 69, 53121 Bonn, Germany*
email: dharam@mpifr-bonn.mpg.de

²*School of Physics, Astronomy, and Mathematics, University of Hertfordshire, Hatfield, UK*
email: mjh@herts.ac.uk

³*Harvard-Smithsonian Center for Astrophysics, MS-67, Cambridge, MA 02138, USA*
email: rkraft@cfa.harvard.edu

⁴*National Centre for Radio Astrophysics (NCRA–TIFR), Pune University Campus, Pune 411 007, India*
email: pramesh@ncra.tifr.res.in

ABSTRACT

X-shaped or winged radio galaxies are those having a pair of low-surface-brightness lobes oriented at an angle to the high-surface-brightness radio lobes. Their nature is a matter of considerable debate; it has even been proposed that they provide evidence for black-hole-mergers/spin-reorientation, and therefore constrain the rate of strong gravitational wave events.

For typical FR II sources, spectral steepening at large distances from the hotspots is well established, but for *X*-shaped sources a variety of spectral behaviour is observed. We propose to compare the spectral behaviour of the low-surface-brightness regions of *X*-shaped sources with similar regions in FR II sources away from the bright jet and hot-spot emission. If the latter show no steepening then the simple picture of electron spectral ageing will need revision; if they do then *X*-shaped sources are indeed peculiar and their formation mechanism will have to be re-examined.

Preliminary results obtained using GMRT observations at 240 MHz and 610 MHz suggest an evidence that low-surface-brightness features for one FR II source shows a flatter spectral index than the high-surface-brightness features, which was also found earlier in some *X*-shaped sources. Further investigations using milliarcsecond-scale imaging and deep X-ray imaging are needed in order to understand the nature of *X*-shaped sources.

1 INTRODUCTION

A peculiar and small subclass of extragalactic radio sources called *X*-shaped, or ‘winged’ sources are characterised by two low-surface-brightness lobes (the ‘wings’) oriented at an angle to the ‘active’, or high surface brightness radio lobes, giving the total source an ‘*X*’ shape. These two sets of lobes usually pass symmetrically through the centre of the associated host galaxy. Merritt & Ekers (2002) noted that the majority of these sources are of Fanaroff-Riley type II (FR II) (Fanaroff & Riley 1974) and the rest are either FR I or mixed.

Formation Scenario Several authors have attempted to explain the unusual structure in *X*-shaped sources. These *X*-shaped radio sources have been put forth as derivatives of central engines that have been reoriented, perhaps due to a minor merger (Merritt & Ekers 2002; Dennett-Thorpe et al. 2002; Gopal-Krishna et al. 2003). Alternatively, they may also result from two pairs of jets, which are associated with a pair of unresolved AGNs (Lal & Rao 2005, 2007). These, however, are not the only interpretations for the unusual morphologies; some authors suggest a hydrodynamic origin (Leahy & Williams 1984; Worrall et al. 1995; Capetti et al. 2002; Kraft et al. 2005) and some suggest a conical precession of the jet axis (Rees 1978; Parma et al. 1985; Mack et al. 1994). See Lal & Rao (2007) and Cheung (2007) for a detailed account.

Observational Implications In several of the formation scenarios mentioned above for X -shaped sources, the wings are interpreted as relics of past radio jets and the active lobes as the newer ones. Hence, the wings or low-surface-brightness features are expected to show steeper spectra than the high-surface-brightness active lobes in standard models for electron energy evolution (‘spectral ageing’). Similarly, in typical FR II radio galaxies, the low-surface-brightness features (regions away from the bright jet and hot-spot emission) are expected to show steeper spectra than the bright jet and/or the hot-spot emission. This can in principle be tested by observation.

2 Source Samples

Known Sample The earlier sample of known X -shaped sources was drawn from the list mentioned in Merritt & Ekers (2002) compiled by Leahy & Parma (1992). There are nearly a dozen such sources, which have been selected solely on the basis of their morphology, and the sample is inhomogeneous and in no sense a statistical complete sample. This sample was observed with the GMRT by Lal & Rao (2007).

Comparison Sample The comparison sample consists of all nearby ($z < 0.1$) normal FR II sources from the 3CRR catalogue. These sources have radio luminosities similar to that of the X -shaped sources, which lie close to the FR I/FR II divide. We impose an angular-size cutoff (based on high-frequency radio maps) on the target sample and ensure that our sample sources are of similar angular size to typical X -shaped sources. The comparison sample thus matches the sample of known X -shaped sources described above. Some of the sample sources have known weak transverse extensions (proto-wings?), similar to the X -shaped sources.

3 GMRT Observations

The 240 MHz and 610 MHz feeds of GMRT (Swarup et al. 1991) are coaxial feeds and therefore, simultaneous multi-frequency observations at these two frequencies are possible. We made synthesis observations of all our sample sources and comparison sample sources at 240 MHz and 610 MHz, in the dual-frequency mode, using the GMRT during several observing GTAC cycles, in the standard spectral-line mode.

The GMRT has a hybrid configuration (Swarup et al. 1991) with 14 of its 30 antennas located in a central compact array with size ~ 1.1 km and the remaining antennas distributed in a roughly ‘Y’ shaped configuration, giving a maximum baseline length of ~ 25 km. The baselines obtained from antennas in the central square are similar in length to the VLA D -array, while the baselines between the arm antennas are comparable in length to the VLA B -array. Hence, a single observation with the GMRT samples the (u, v) plane adequately on the short baselines as well as on the long baselines and provides good angular resolution when mapping the detailed source structure with reasonably good sensitivity.

3.1 Data Reduction

The visibility data were converted to FITS and analyzed using standard AIPS. The flux calibrators 3C 48, 3C 147 and 3C 286 were observed depending on the availability either at the beginning and/or at the end as an amplitude calibrator and to estimate and correct for the bandpass shape. We used for the flux-density scale an extension of the Baars et al. (1977) scale to low frequencies, using the coefficients in AIPS task ‘SETJY’. The secondary phase calibrators were observed at intervals of ~ 30 min. The error in the estimated flux density, both due to calibration and systematic, is $\leq 5\%$. The data suffered from scintillations and intermittent radio frequency interference (RFI). In addition to normal editing of the data, the scintillations affected data and channels affected due to RFI were identified and edited, after which the central channels were averaged using

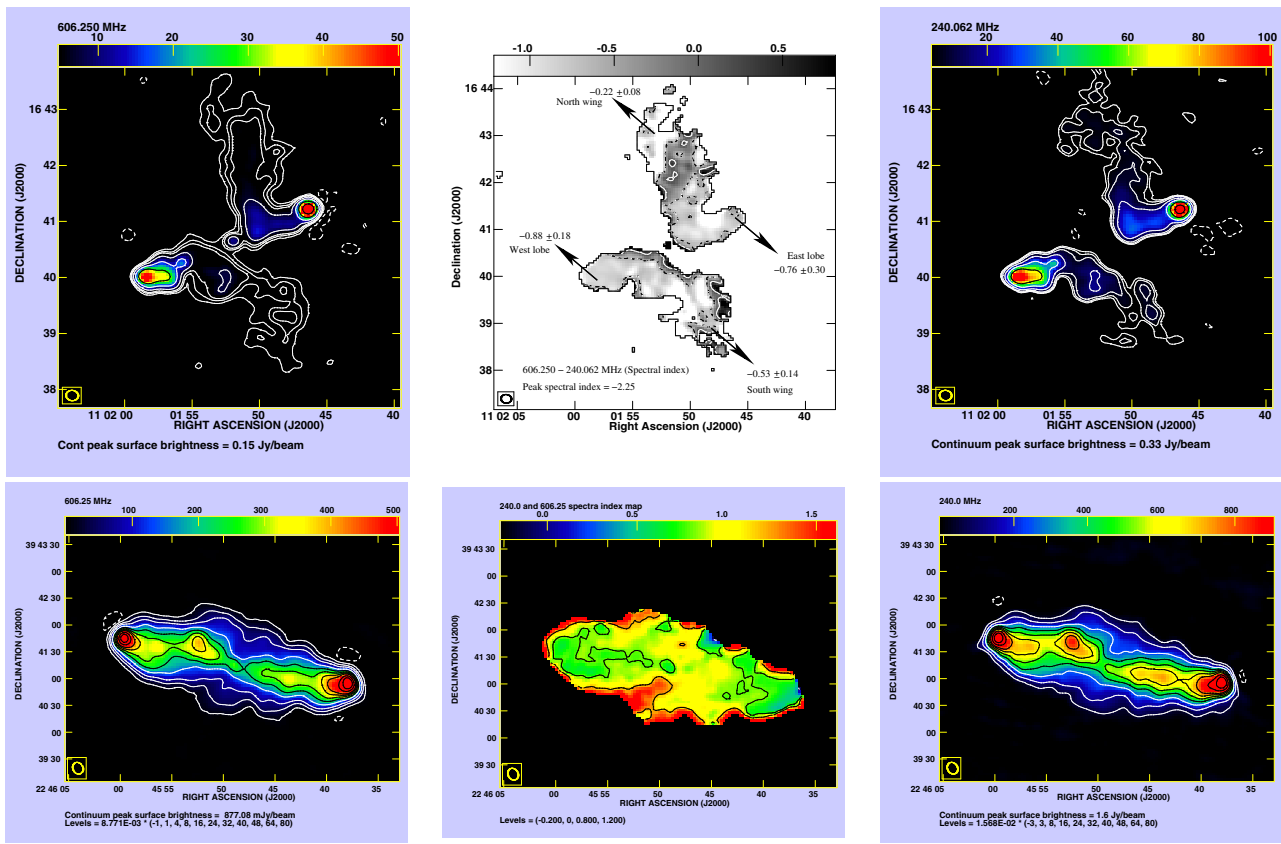


Figure 1: GMRT map of B1059+169 (a known X-shaped source in the Abell 1145 cluster) at 610 MHz (top left panel), 240 MHz (top right panel) and the spectral index (240 MHz, 610 MHz) map (top middle panel). Similarly, the lower panel shows the GMRT map of 3C 452 (a FR II source, possibly missed from the X-shaped sample due to projection), from our comparison sample at 610 MHz (bottom left panel), 240 MHz (bottom right panel) and the spectral index (240 MHz, 610 MHz) map (bottom middle panel). Although, the uniformly weighted CLEAN beams for 610 MHz and 240 MHz arrays are $\sim 6''$ and $\sim 15''$, respectively, the GMRT data at 610 MHz were tapered to produce a map matched with the resolution of 240 MHz. Note the unusual spectral index (flux density, $S_\nu \propto \nu^\alpha$, where ν and α are the frequency and the spectral index, respectively,) in B1059+169.

the AIPS task ‘SPLAT’ to reduce the data volume. To avoid bandwidth smearing, the effective band width at 240 MHz and 610 MHz was reduced to five and three channels, respectively.

While imaging, 49 facets spread across a ~ 3.24 square degree field were used at 240 MHz and 9 facets covering slightly less than a 0.5 square degree field, were used at 610 MHz to map each of the two fields using the AIPS task ‘IMAGR’. To make high-resolution images that are also sensitive to extended structure, we have employed the SDI CLEANing algorithm (Steer et al. 2003). We used uniform weighting and the 3D option for w -term correction throughout our analysis. The presence of a large number of point sources in the field allowed us to do phase self-calibration to improve the image. After two or three cycles of phase self-calibration, a final self-calibration of both amplitude and phase was made and the final image was produced. At each iteration of self-calibration, the Fourier transform of the image and the visibilities were compared to check for the improvement in the source model. The final images (see Fig. 1) were stitched together using the AIPS task ‘FLATN’ and corrected for the primary beam of the GMRT antennas.

4 RESULTS

Known *X*-Shaped sources The spectral characteristics of known *X*-shaped sources seem to fall into three distinct categories, namely, sources in which (i) the wings have flatter spectral indices than the active lobes, (ii) the wings and the active lobes have comparable spectral indices, and (iii) the wings have steeper spectral indices than the active lobes.

Comparison FR II sources We find evidence for the presence of possible unusual spectral properties in typical FR II radio galaxies; *i.e.*, from the study of our comparison sample of FR II radio sources, one source from our sample seems to have relatively flatter spectral indices for the low-surface-brightness features than the high-surface-brightness features.

CONCLUSIONS While it is equally probable that the three categories, (i), (ii) & (iii), of *X*-shaped sources are unrelated to one another, a single model to explain these sources is a challenge. Currently a strong contender to explain the ‘*X*’ shape morphology and thus the formation scenario is the ‘alternative’ model of Lal & Rao (2007), in which the *X*-shaped sources consist of two pairs of jets, which are associated with two unresolved AGNs. However, since classical FR II radio galaxies also show unusual spectral behaviour, it seems that the simple picture of electron spectral ageing will also need revision.

Acknowledgments

We thank the staff of the GMRT who have made these observations possible. GMRT is run by the National Centre for Radio Astrophysics of the Tata Institute of Fundamental Research. DVL is grateful to R. Nityananda for discussions and several useful comments. DVL thanks A.L. Roy for his careful reading of the manuscript and his comments.

References

- [1] Dennett-Thorpe, J., Scheuer, P.A.G., Laing, R.A., Bridle, A.H., Pooley, G.G., Reich, W., 2002, MNRAS, 330, 609
- [2] Ekers, R.D., Fanti, R., Lari, C., Parma, P., 1978, Nature, 276, 588
- [3] Fanaroff, B.L., Riley J.M., 1974, MNRAS, 167, 31P
- [4] Kraft, R.P., Hardcastle, M.J., Worrall, D.M., Murray, S.S., 2005, ApJ, 622, 149
- [5] Lal, D.V. & Rao, A.P., 2005, MNRAS, 356, 232
- [6] Lal, D.V. & Rao, A.P., 2007, MNRAS, 374, 1085
- [7] Leahy, J.P., Parma, P., 1992 in Roland, J., Sol, H., Pelletier, G, eds, Extragalactic Radio Sources. From Beams to Jets, Cambridge University Press, p. 307
- [8] Merritt, D. & Ekers, R.D., 2002, Sci, 297, 1310
- [9] Swarup, G., Ananthakrishnan, S., Kapahi, V.K., Rao, A.P., Subrahmanya, C.R., Kulkarni, V.K., 1991, Cu. Sc., 60, 95
- [10] Worrall, D.M., Birkinshaw, M., Cameron, R.A., 1995, ApJ, 449, 93